Thom, R., Sivakumar, R., Sivakumar, V., Murray, E. J. & Mackinnon, P. (2007). *Géotechnique* **57**, No. 5, 469–474

TECHNICAL NOTE

Pore size distribution of unsaturated compacted kaolin: the initial states and final states following saturation

R. THOM*, R. SIVAKUMAR†, V. SIVAKUMAR*, E. J. MURRAY‡ and P. MACKINNON*

KEYWORDS: collapse settlement; compaction; expansive soils; partial saturation; suction

INTRODUCTION

The structure of soil is derived from the arrangement of the particles, and affects the overall mechanical and hydro-mechanical properties (Casagrande, 1932; Lambe, 1951; Mitchell, 1976; Leroueil & Vaughan, 1990). Within the context of fine-grained unsaturated soils, different structures result from compaction depending on whether water contents are wet or dry of optimum, and they significantly affect the performance of unsaturated soils (Barden & Sides, 1970, Alonso *et al.*, 1995; Gens *et al.*, 1995; Lloret *et al.*, 2003; Romero *et al.*, 2003). Generally, a flocculated structure develops when fine materials are compacted at water contents dry of optimum. Flocculation is synonymous with the development of aggregates of soil particles with an inherent bimodal pore size distribution (Fig. 1). The bimodal distribution of void space refers to the microstructural or intra-aggregate voids within the particle aggregates, and the macrostructural or inter-aggregate void spaces between the aggregates determined by their position, orientation and shape.

Techniques such as mercury intrusion porosimetry (MIP) have been used to demonstrate the bimodal pore size distribution of unsaturated soil. The distribution of the pore sizes both within and between the aggregates is influenced by the way the unsaturated soil is formed. Delage *et al.* (1996) and Lloret *et al.* (2003) reported the effects of bulk density and compaction effort on pore size distribution. Studies have also been reported on the influence of compaction water content on the pore size distribution. However, little or no information is available on how pore size distribution is affected by saturation of a soil following preparation under unsaturated conditions. This is the main thrust of this technical note, which also reports on the pore size distributions of samples of kaolin prepared using different preparation techniques and compaction efforts. These latter results are used to explain the phenomena observed on wetting.

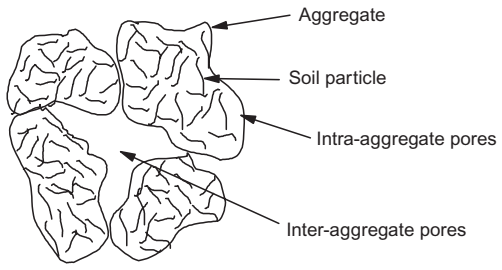

Fig. 1. Aggregate structure

Manuscript received 20 February 2006; revised manuscript accepted 6 March 2007.
Discussion on this paper closes on 3 December 2007, for further details see p. ii.
* Queen's University Belfast, Northern Ireland.
† WS Atkins, Epsom, London, UK.
‡ MurrayRix Geotechnical, Stoke Golding, UK.

LABORATORY EXPERIMENTS

Sample preparation

A series of experiments was carried out to investigate the effect of post-compaction wetting, compaction water content, method of compaction and compactive effort on the existence of a bimodal pore distribution in samples of speswhite kaolin clay. In preparing unsaturated samples, 2 kg of kaolin was mixed with de-aired water to achieve the water contents of 22·5%, 25% or 27·5%. These are all dry of the optimum water content for kaolin of around 29% based on standard Proctor compaction. The mixed material was passed through a sieve of 1·18 mm aperture size, with any material not passing through the sieve broken down and re-sieved. The authors acknowledge that sieving limited the maximum size of inter-aggregate pores, but it ensured a consistent, homogeneous soil mixture. The sieved material was stored in plastic bags in a temperature-controlled room for two days to allow moisture equilibrium. The samples for testing were prepared using three different methods, as follows.

Isotropic compression Isotropically compressed samples were prepared using a standard triaxial cell suitable for testing 100 mm diameter samples. In this system a rubber membrane was placed around the pedestal and sealed to the base using two O-rings. A membrane stretcher was placed around the membrane, and the top of the membrane was folded over the top of the stretcher. The sieved material was placed slowly into the membrane, a top cap with dry porous stone was fitted, and the membrane was unfolded. The membrane stretcher was then removed and the top cap was sealed with two O-rings. The cell was assembled and pressurised to 400 kPa, 800 kPa or 1050 kPa using compressed air. Any air pressure in the sample, developed as a result of the application of the external pressure, was allowed to vent from the top and bottom taps. Although the consolidation usually took place quickly, the sample was left in the compression system for 3 days as a standard procedure. At the end of this time the confining pressure was reduced to zero and a 50 mm diameter sampler was used to obtain a 100 mm long sample. For further details refer to Sivakumar (2005).

Static compression Samples were compressed in nine layers into a 50 mm diameter split compaction mould 140 mm high. Each layer was statically compressed into the compaction

mould by compressing the material at a fixed displacement rate of 1·5 mm/min. The compression was terminated when a target vertical pressure of 400 kPa or 800 kPa or 1200 kPa was achieved.

Dynamic compaction The split compaction mould (50 mm in diameter and 140 mm high) was used to produce the dynamically compacted samples. The sieved material was placed in the split mould in nine layers, and each layer was compacted with nine blows from a hammer mass of mass 175 g with a 25 mm diameter base falling through a height of 300 mm.

Wetting and consolidation procedures

Samples compressed isotropically to initial pressures of 400 kPa and 800 kPa were allowed to saturate under an effective confining pressure of 37·5 kPa using the procedure reported by Sivakumar (2005). The volume change of the samples during this process was measured using the twin-cell arrangement developed by Sivakumar *et al.* (2006). At the end of the wetting process the samples were unloaded under undrained conditions for MIP investigation.

Mercury intrusion porosimetry

Small cubic specimens of approximately 10 mm side were carefully cut from the samples prepared using the various procedures described above. The prepared specimens were freeze-dried using the method described by Ahmed *et al.* (1974), which involved quick freezing of the soil specimen to cryogenic temperatures below −130°C, to avoid formation of crystalline ice, by direct immersion in liquid nitrogen. Following freezing, the water in the specimens was removed by sublimation using a true vacuum at a temperature between −60°C and −80°C. This process of dehydration prevents air/water menisci from forming as the water is removed. The freeze-dried specimens were wrapped in cling-film and kept in airtight plastic bags prior to carrying out the MIP tests (D 4404-84; ASTM, 1984), which were performed in the geotechnical laboratory of Durham University. The mercury chamber was initially calibrated for apparent volume change by pressurising the chamber to 6120 kPa in steps (a step of 68 kPa up to 680 kPa and then a step of 680 kPa up to 6120 kPa). A similar procedure was repeated when the sample was in the mercury chamber, and each pressure increment was maintained constant until no significant volume of mercury entered into the chamber. The difference between the two volume change measurements is assumed to be the volume of mercury intruded into the pores of the dry kaolin sample at the specified pressure. The pore diameters were calculated using the equation proposed by Washburn (1921):

$$p = \frac{-4\gamma \cos\theta}{d} \tag{1}$$

where θ and γ are the contact angle and surface tension respectively. Two different illustrations are used for the discussion presented in this paper: (a) incremental pore volume (i.e. volume of mercury intruded into the sample between consecutive pressure increments) per gram of dry kaolin; and (b) cumulative volume change per gram of dry kaolin with respect to pore size.

RESULTS AND DISCUSSION

The paper is aimed primarily at examining the effects of post-preparation saturation on the pore size distribution of initially unsaturated soils, and the discussion of the findings follows an overview of the general pore size distribution of unsaturated soils resulting from various sample preparation methods.

Effect of moisture content, type of compaction and compaction pressure on pore size distribution of unsaturated soils

Figures 2, 3 and 4 illustrate the pore size distributions based on the MIP tests of samples that were isotropically compressed, statically compressed and dynamically compacted at moisture contents of 22·5%, 25% and 27·5%. The plots indicate the incremental pore volume for 1 g of dry

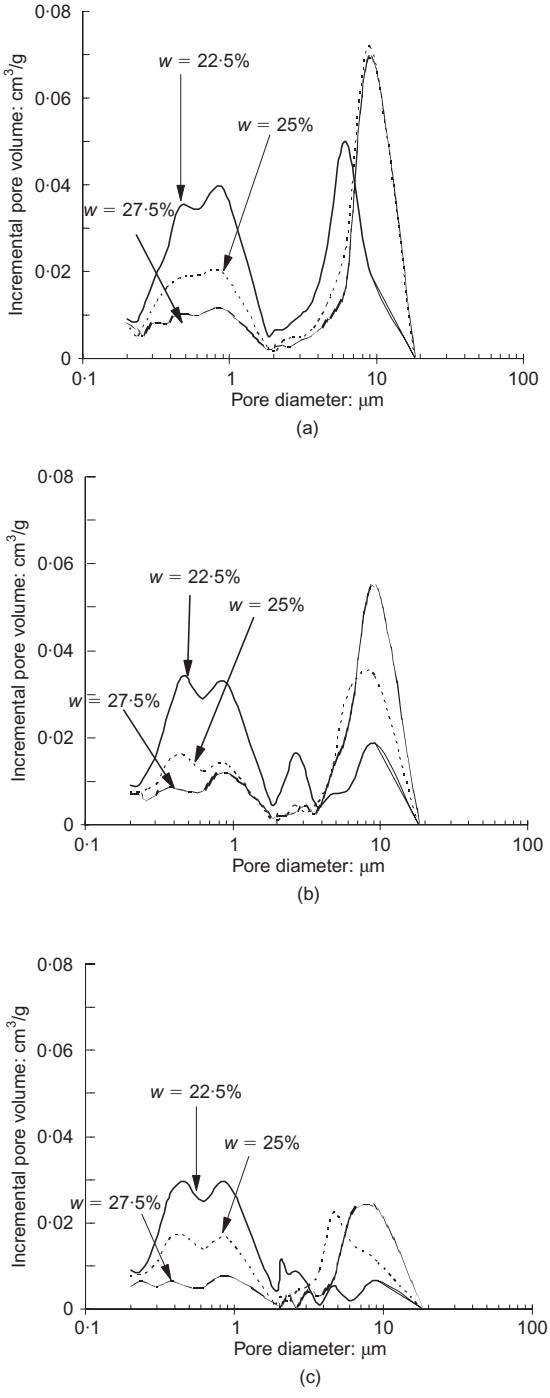

Fig. 2 Pore size distribution of samples isotropically compressed to various pressures at water contents of 22·5%, 25% and 27·5%: (a) 400 kPa; (b) 800 kPa; (c) 1050 kPa

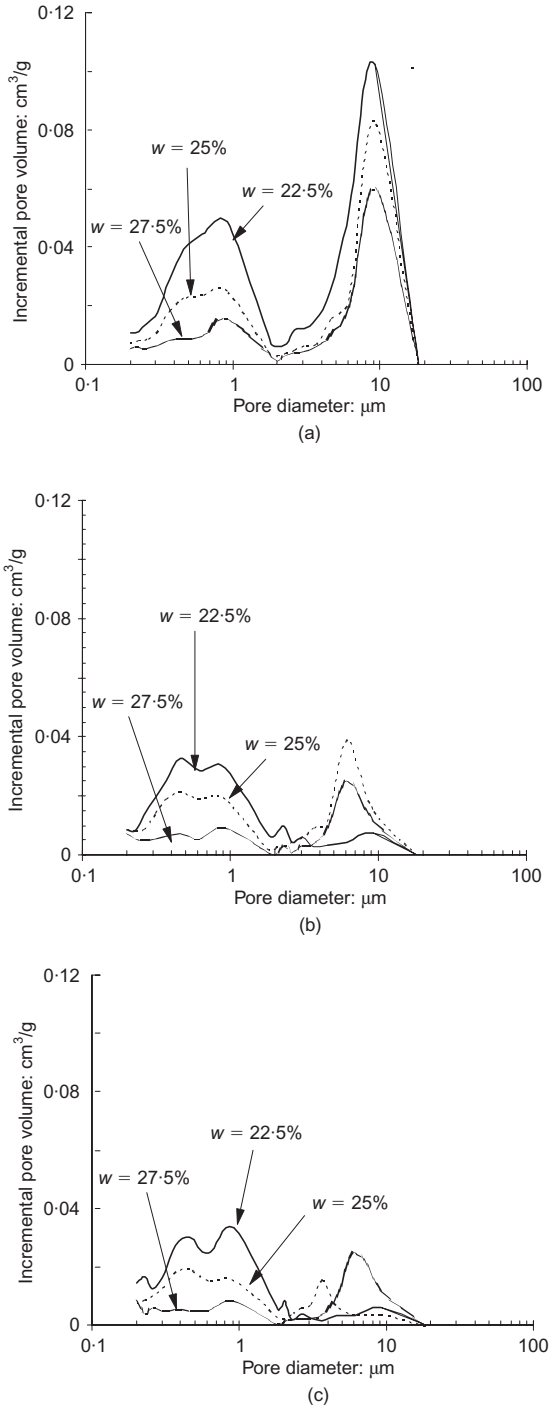

Fig. 3. Pore size distribution of samples statically compressed to various pressures at water contents of 22·5%, 25% and 27·5%: (a) 400 kPa; (b) 800 kPa; (c) 1050 kPa

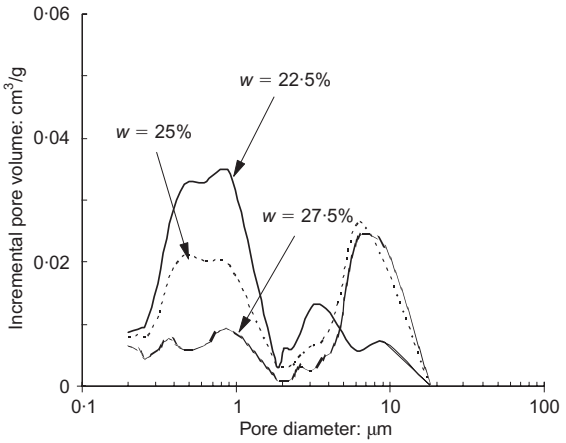

Fig. 4. Pore size distribution of samples dynamically compacted at water contents of 22·5%, 25% and 27·5%

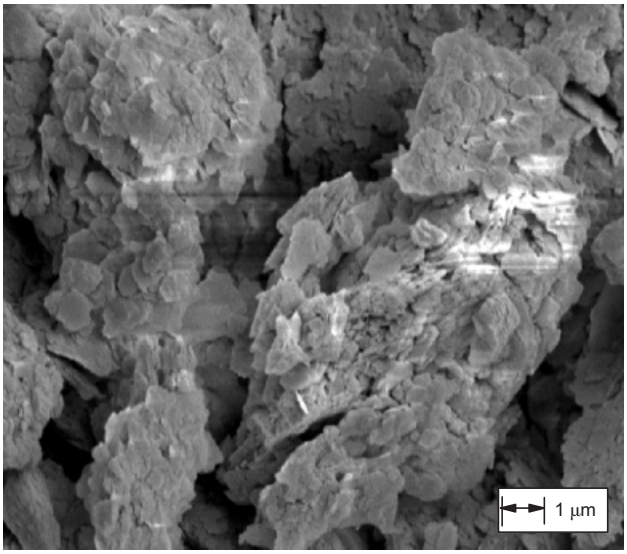

Fig. 5. SEM image of sample of compacted kaolin (static compression to 800 kPa at water content of 25%)

kaolin sample plotted against the pore diameter. Incremental pore volume refers to the volume of mercury that intrudes into the pores between pressure increments. Irrespective of the method of sample preparation there is clear indication of the existence of a bimodal pore distribution in the unsaturated soils. This is pictorially illustrated in Fig. 5 by the scanning electron microscope (SEM) image taken of one of the specimens isotropically compressed. The plots indicate a distinct division between those smaller voids interpreted as constituting the intra-aggregate pore spaces and the larger inter-aggregate voids. The intra-aggregate voids are typically between 0·3 μm and 2 μm, with the larger inter-aggregate voids being $>$ 3 μm and typically around 10 μm. Thus the intra-aggregate voids are around 10–20 times larger than the voids within the aggregations. The division between the two sets of void spaces of 2–3 μm corresponds approximately to the particle size of kaolinite. In general, the lower the compaction water content, the greater the percentage of the intra-aggregate pores and the less the inter-aggregate pores, though it is recognised that the percentage of inter-aggregate pores for the drier soils may be influenced by macro-fissures not being represented in the small samples tested.

Both compression pressure (isotropic or static pressure) and water content at the time of compression influence the pore size distribution in the unsaturated soils. While Fig. 4 cannot be used to appraise the significance of different dynamic compactions, as only a single hammer mass was used, the form of the pore size distributions is similar to those for the isotropic and statically compressed samples. At a given water content the increase in compression pressure in Figs 2 and 3 has an effect on both the intra-aggregate and inter-aggregate pores, although the influence on the former is more pronounced.

For the isotropically compressed samples in Fig. 2, at the compression water content of 22·5%, the peak incremental pore volume for the intra-aggregate pores is shown as approximately 0·04 cm^3/g, which reduces to 0·036 cm^3/g and 0·03 cm^3/g when the compression pressure is increased to 800 kPa and 1050 kPa respectively. Similarly, the incremen-

tal pore volumes at the compression water content of 25% are 0·02 cm^3/g, 0·015 cm^3/g and 0·015 cm^3/g for increasing compressive effort. In this case the effects of compression pressure on the intra-aggregate pore size distribution are not as significant. When the compression water content is 27·5% the change in the intra-aggregate pore size distribution as a result of the increase in compression pressure is insignificant. This may be explained by noting that at the higher water content of 27·5% the specimens were only around 1·5% less than the optimum water content (based on standard Proctor compaction). The aggregates may be considered saturated even before the application of the compression process. However, since the pore water pressure in the aggregates was negative, the application of compression pressure will not have led to expulsion of water from the aggregates, and their volume can be expected to have remained virtually unchanged during compression. However, at the water content of 22·5% the specimens were well below the plastic limit of kaolin (PL = 34%) and approximately 5% less than the optimum water content. The reduction in intra-aggregate voids under increasing compressive stress suggests there is disturbance of the aggregates and rearrangement of the soil particles at this low water content. This would be consistent with a brittle, possibly fissured, aggregate structure.

Figure 3 shows the bimodal pore size distributions obtained on samples of kaolin statically compressed. The plots show a reduction in the intra-aggregate pore volume due to increasing pressure at all water contents, although the higher the water content the less the effect. The observation differs from the findings for those samples that were isotropically compressed. One-dimensional compression has a shearing action and would appear to lead to greater aggregate disturbance and particle rearrangement under compression, consistent with an inferred brittle structure.

The volumes of the inter-aggregate pores at the higher water contents are generally, though not consistently, greater than those for the lower water contents, irrespective of the preparation procedure. This is the reverse of the observation for the intra-aggregate pores. The results also indicate that the magnitude of inter-aggregate pore volumes is significantly reduced by increasing pressure for both isotropic and statically compressed specimens. In the case of isotropic compression (Fig. 2), for the water content of 22·5%, the maximum incremental pore volume is shown as approximately 0·05 cm^3/g for a compression pressure of 400 kPa, but reduces to 0·02 cm^3/g and 0·005 cm^3/g for compression pressure increases to 800 kPa and 1050 kPa respectively. This indicates large reductions in the inter-aggregate pore volume with increasing compressive pressure. For compression water content increase to 25·0% and 27·5% similar observations may be made. For the water content of 27·5% the increase in compression pressure reduces the maximum inter-aggregate pore volume from 0·07 cm^3/g to 0·03 g/cm^3. This implies that the occurrence of a bimodal pore size distribution may not be destroyed by compressing samples to high pressure, even if the material was prepared at only a little less than optimum water content. Similar conclusions may be reached for those samples prepared using static compression in Fig. 3.

Influence of wetting on pore size distribution

Two isotropically compressed samples, one compressed to 400 kPa and the other to 800 kPa, were subsequently saturated at a mean effective pressure of 37·5 kPa. The specific volumes after compression were 2·20 and 1·99 respectively at a compression water content of 25·0% for both samples. The samples will be referred to as S400 and S800. The initial suction in the samples was about 1000 kPa (Sivakumar, 2005) and was reduced to zero on saturation and swelling. Fig. 6 shows the changes in the specific volume plotted against suction for both samples.

The specific volume of sample S400 increased from 2·20 to 2·28 for the reduction in suction from 1000 kPa to zero. For S800 the specific volume showed a corresponding increase from 1·99 to 2·16. Alonso *et al.* (1990) proposed the following equation for evaluating the elastic volume change δv resulting from a change in suction ds, where κ_s is the swelling gradient with respect to suction s when plotted in logarithmic scale.

$$\delta v = -\kappa_s \frac{\mathrm{d}s}{s + p_{atm}} \tag{2}$$

where p_{atm} is reference pressure. According to Alonso *et al.* (1990) the magnitude of κ_s of samples prepared at similar water contents but with different initial specific volumes should be the same if the wetting path (reduction of suction) remains inside the loading collapse (LC) yield locus. However, referring to Fig. 6, the increase in specific volume for S800 of 0·17 is approximately twice as great as the increase for S400 of 0·08, and consequently κ_s differs significantly for the different compression pressures used in the sampling process and thus the initial specific volumes. The reason for this difference may be explained by examining the MIP results of Fig. 7.

Figure 7 shows the pore size distributions for samples S400 and S800 taken through the wetting process. The figure shows the initial pore size distributions S400(i) and S800(i) prior to wetting and the corresponding distributions S400(s) and S800(s) after saturation. The maximum incremental pore volume of inter-aggregate pores, in the case of S400, is shown as approximately 0·08 cm^3/g at a pore size of 10 μm, and is shown as reducing to 0·02 cm^3/g at the same pore size following saturation. In the case of S800 the maximum incremental inter-aggregate pore volume is shown as 0·04 cm^3/g at a pore size of 10 μm, reducing to approximately 0·018 cm^3/g on saturation. While the inter-aggregate pore size remains virtually unchanged, the percentage of intra-aggregate pores is significantly increased by wetting.

Swelling of the samples is generated by the expansion of the aggregates instigated by the uptake of water and reduction in suction. If the overall volume increase of the sample matches the swelling of the aggregates, the inter-aggregate pore volume would be expected to remain unchanged. This is graphically illustrated in Fig. 8(a). Inflatable irregular

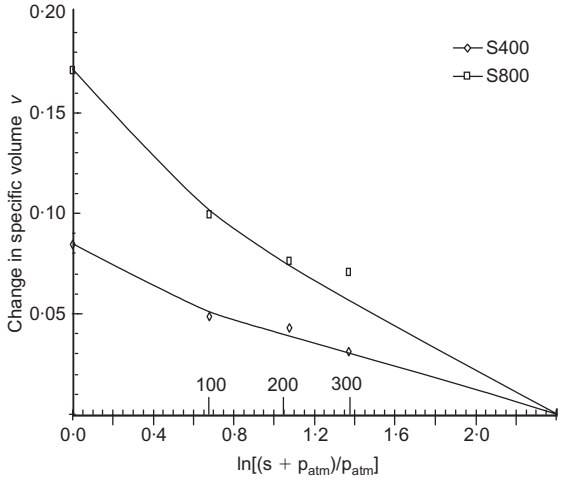

Fig. 6. Change in specific volume of samples subjected to wetting

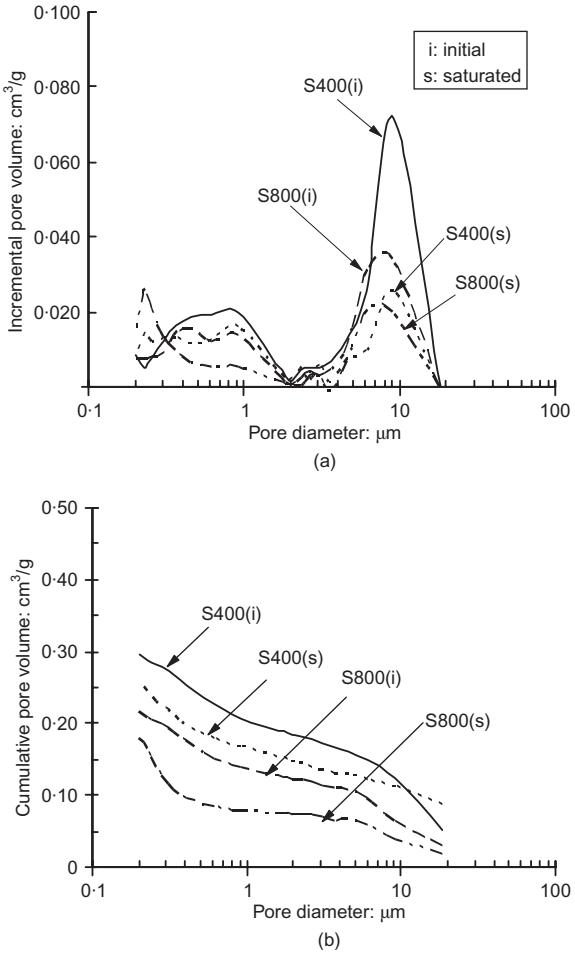

Fig. 7. Pore size distribution of samples subjected to wetting: (a) incremental pore volume; (b) cumulative pore volume

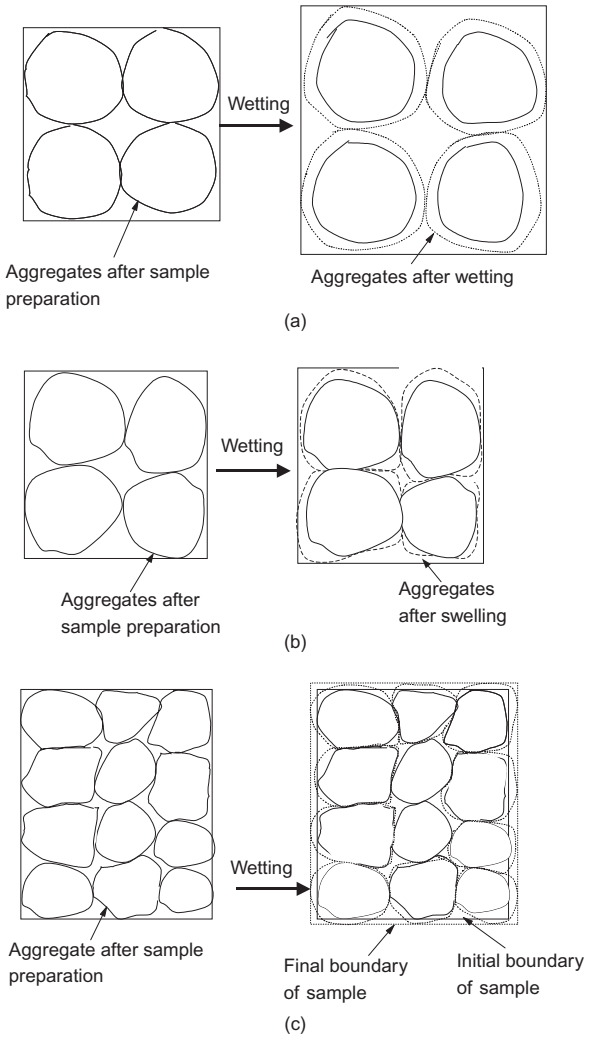

Fig. 8. Schematic illustration of aggregates response to wetting: (a) no aggregate expansion into macro void spaces; (b) lightly packed aggregates (aggregate expansion into macro void spaces); (c) densely packed aggregates

balls, which represent the aggregates, are packed in a box that has flexible boundaries. As the balls expand, the boundary of the external box would be expected to move outwards with the overall volume increase, and the percentage increase will be the same as the percentage volume increase of the aggregates; the same argument applies to the volume of the void space between the balls. However, according to the MIP tests on samples S400 and S800 there was a significant reduction in the inter-aggregate volumes. This can only be explained by aggregate expansion into the inter-aggregate pore spaces. This is graphically presented in Fig. 8(b), and suggests that the aggregates behave as deformable structures in which particle rearrangement takes place under changing conditions.

The ability of the aggregates to expand into the inter-aggregate pore spaces depends on how tightly the aggregates are packed as a result of the initial compression. This means that the aggregates of S800 can be expected to have experienced greater resistance to swelling into the inter-aggregate pore spaces than the aggregates of S400, as there is less inter-aggregate pore space when the aggregates are tightly packed. Consequently this results in a larger overall increase in volume. This is graphically illustrated in Fig. 8(c). This is consistent with sample S800 exhibiting less reduction in inter-aggregate pore volume in Fig. 7 and consequently greater increase in overall sample volume than S400, as reported in Fig. 6. The behaviour described explains the change in specific volume for S800 of 0·17 compared with the change for S400 of 0·08 on saturating the samples, even though the samples were prepared at the same water content.

CONCLUSIONS

Tests were carried out to investigate the effect of compaction water content, compaction effort, compaction type and post-compaction wetting on the pore size distributions of unsaturated kaolin. The pore size distributions of freeze-dried samples were determined using mercury intrusion porosimetry (MIP). The results were as follows.

(*a*) A difference of as little as 2·5% in compaction water content resulted in significant differences in pore size distribution for samples that underwent an identical compression/compaction procedure.

(*b*) There was a clear indication of a bimodal pore size distribution and division between those smaller voids interpreted as constituting the intra-aggregate pore spaces and the larger inter-aggregate voids. The intra-aggregate voids were around 10 to 20 times larger than those of the voids within the aggregations.

(*c*) Though not consistent for all samples, in general the lower the compaction water content the greater the percentage of the intra-aggregate pores and the fewer the inter-aggregate pores.

(*d*) Increasing compressive pressure, whether isotropic or static, resulted in a considerable reduction in the inter-aggregate pore volume, but also resulted in a reduction

in the intra-aggregate pore spaces, particularly of those samples prepared at low water content.

(*e*) Importantly, the bimodal structure was not broken down by compaction, even at water contents close to the optimum.

(*f*) The wetting of unsaturated samples resulted in individual aggregates expanding into the inter-aggregate void spaces, reducing the overall potential expansion of the sample. The greater the initial compaction, the denser the sample and the less the closure of the inter-aggregate voids, and the greater the overall sample expansion, for a given increase in water content. The aggregates thus act as deformable structures in which particle rearrangement takes place under changing conditions.

ACKNOWLEDGEMENTS

Funding for the work was provided by Glover Site Investigations Ltd, Country Antrim, Northern Ireland. The authors thank Dr D. Toll for providing facilities for performing the MIP tests at the geotechnical testing laboratory in Durham University. The authors also thank VJ Tech Ltd, UK.

NOTATION

d	pore size
PL	plastic limit
p	pressure of mercury
p_{atm}	reference pressure
q	contact angle
s	suction
v	specific volume
δ	small change
γ	surface tension
κ_s	swelling gradient with respect to suction

REFERENCES

Ahmed, S., Lovell, C. W. J. & Diamond, S. (1974). Pore sizes and strength of compacted clay. *J. Soil Mech. Found. Div. ASCE* **100**, No. 4, 407–425.

Alonso, E. E., Gens, A. & Josa, A. (1990). A constitutive model for partially saturated soils. *Géotechnique* **40**, No. 3, 405–430.

Alonso, E. E., Lloret, A., Gens, A. & Yang, D. Q. (1995). Experimental behaviour of highly expansive double-structure clay. *Proc. 1st Int. Conf. on Unsaturated Soil, Paris* **1**, 11–16.

ASTM (1984). *Standard test method for determination of pore volume and pore volume distribution of soil and rock by mercury intrusion porosimetry*, D4404-84. West Conshohocken, PA: ASTM International.

Barden, L. & Sides, G. R. (1970). Engineering behaviour and structure of compacted clay. *J. Soil Mech. Found. Engng ASCE* **96**, No. SM4, 1171–1201.

Casagrande, A. (1932). The structure of clay and its importance in foundation engineering. In *Contributions to Soil Mechanics, 1925–1940*, pp. 72–113. Boston Society of Civil Engineers.

Delage, P., Audiguier, M., Cui, Y.-J. & Howat, M. D. (1996). Microstructure of a compacted silt. *Can. Geotech. J.* **33**, 150–158.

Gens, A., Alonso, E. E, Suriol, J. & Lloret, A. (1995). Effect of structure on the volumetric behaviour of a compacted soil. *Proc. 1st Int. Conf. on Unsaturated Soils, Paris*, 83–88.

Lambe, T. W. (1951). The structure of compacted clay. *J. Soil Mech. Found. Div. ASCE* **84**, No. SM2, 1–34.

Leroueil, S. & Vaughan, P. R. (1990). The general and congruent effects of structure in natural soils and weak rocks. *Géotechnique* **40**, No. 3, 467–488.

Lloret, A., Villar, M. V., Sanchez, M., Gens, A., Pimtado, X. & Alonso, E. E. (2003). Mechanical behaviour of heavily compacted bentonite under high suction changes. *Géotechnique* **53**, No. 1, 27–40.

Mitchell, J. K. (1976). *Fundamentals of soil behavior*. New York: John Wiley & Sons.

Romero, E., Gens, A. & Lloret, A. (2003). Suction effects on a compacted clay under non-isothermal conditions. *Géotechnique* **53**, No. 1, 65–81.

Sivakumar, R. (2005). *Effects of anisotropy on the behaviour of unsaturated clay.* PhD thesis, Queen's University Belfast.

Sivakumar, R., Sivakumar, V., Blatz, J. & Vimalan, J. (2006). Twin-cell stress-path apparatus for testing unsaturated soils. *Geotech. Test. J.* **29**, No. 3, 1–5.

Washburn, E. W. (1921). Note on a method of determining the distribution of pore sizes in a porous material. *Proc. Nat. Acad. Sci. US* **7**, 115–116.